INFECTION AND IMMUNITY, Oct. 2006, p. 5433–5444 Vol. 74, No. 10
0019-9567/06/$08.00+0 doi:10.1128/IAI.00052-06

Major Role for FeoB in *Campylobacter jejuni* Ferrous Iron Acquisition, Gut Colonization, and Intracellular Survival

Hemant Naikare,[1] Kiran Palyada,[1] Roger Panciera,[1] Denver Marlow,[2] and Alain Stintzi[1,3]*

Department of Veterinary Pathobiology, College of Veterinary Medicine, Oklahoma State University, Stillwater, Oklahoma 74078[1]; Department of Physiological Sciences, College of Veterinary Medicine, Oklahoma State University, Stillwater, Oklahoma 74078[2]; and Department of Biochemistry, Microbiology, and Immunology, Faculty of Medicine, University of Ottawa, 451 Smyth Road, Ottawa, Ontario K1H 8M5, Canada[3]

Received 10 January 2006/Returned for modification 21 March 2006/Accepted 12 July 2006

To assess the importance of ferrous iron acquisition in *Campylobacter* physiology and pathogenesis, we disrupted and characterized the Fe^{2+} iron transporter, FeoB, in *Campylobacter jejuni* NCTC 11168, 81-176, and ATCC 43431. The *feoB* mutant was significantly affected in its ability to transport $^{55}Fe^{2+}$. It accumulated half the amount of iron than the wild-type strain during growth in an iron-containing medium. The intracellular iron of the *feoB* mutant was localized in the periplasmic space versus the cytoplasm for the wild-type strain. These results indicate that the *feoB* gene of *C. jejuni* encodes a functional ferrous iron transport system. Reverse transcriptase PCR analysis revealed the cotranscription of *feoB* and Cj1397, which encodes a homolog of *Escherichia coli feoA*. *C. jejuni* 81-176 *feoB* mutants exhibited reduced ability to persist in human INT-407 embryonic intestinal cells and porcine IPEC-1 small intestinal epithelial cells compared to the wild type. *C. jejuni* NCTC 11168 *feoB* mutant was outcompeted by the wild type for colonization and/or survival in the rabbit ileal loop. The *feoB* mutants of the three *C. jejuni* strains were significantly affected in their ability to colonize the chick cecum. And finally, the three *feoB* mutants were outcompeted by their respective wild-type strains for infection of the intestinal tracts of colostrum-deprived piglets. Taken together, these results demonstrate that FeoB-mediated ferrous iron acquisition contributes significantly to colonization of the gastrointestinal tract during both commensal and infectious relationship, and thus it plays an important role in *Campylobacter* pathogenesis.

The ferrous iron transporter was isolated for the first time in *Escherichia coli*, more than 15 years ago, by Hantke (12). The two *E. coli* genes, *feoA* and *feoB*, were then fully characterized and sequenced by Kammler and coworkers 6 years later (14). *E. coli* mutants of both genes were shown to be significantly affected in their ability to transport ferrous iron (14). During the past 10 years, the ferrous iron acquisition system has been experimentally identified in seven additional microbes: *Porphyromonas gingivalis* (6), *Leptospira biflexa* (16), *Helicobacter pylori* (35), *Shigella flexneri* (27), *Salmonella enterica* serovar Typhimurium (4, 33), *Legionella pneumophila* (26), and the cyanobacterium *Synechocystis* sp. (15). Interestingly, the FeoB-mediated ferrous iron acquisition has been found to play an essential role in bacterial virulence (4, 6), intracellular survival (26, 27), replication in macrophage (4), and/or gastrointestinal tract colonization (32, 33, 35).

In *E. coli*, the *feoA* and *feoB* genes are organized in an operonic structure with a third gene named *feoC* (11). The genes *feoA* and *feoC* encode two small proteins of 75 and 78 amino acids, respectively. The function of these proteins in ferrous iron transport is still unknown. The *feoB* gene encodes an integral cytoplasmic membrane protein of 773 amino acids. FeoB homologs are found in all bacterial kingdoms from *Archaea* to gram-positive and gram-negative bacteria (11). Interestingly, the FeoB protein shares homology with GTP-binding proteins. It contains four of the five GTPase signature motifs. Mutational and GTP binding studies have demonstrated the requirement of GTP/GDP binding for ferrous iron uptake (18). Although it is clear that FeoB is required for ferrous iron acquisition, its precise function in iron transport and whether or not FeoB binds iron is not known (11, 18).

Campylobacter jejuni is a major etiological agent of gastroenteritis worldwide and causes up to 2.5 million illnesses every year in the United States alone (19). This pathogen colonizes primarily the gastrointestinal tract of warm-blooded animals. The oxygen-reduced environment of the gut will likely favor the reduction of iron to its ferrous state. Consequently, ferrous iron might be an important iron source for enteric pathogens such as *C. jejuni* given that *feoB* mutants of *E. coli*, *H. pylori*, and *S. enterica* serovar Typhimurium, have been shown to be attenuated in their ability to colonize the host gastrointestinal tract (32, 33, 35). The analysis of the *C. jejuni* NCTC 11168 genome reveals that it carries an *feoAB*-like operon (21). The *C. jejuni* FeoB protein shares 50% identity and 69% similarity at the amino acid level with the FeoB protein of *H. pylori*. Surprisingly, and in contrast to all of the other studied and characterized FeoB proteins, the FeoB homolog in *C. jejuni* was recently found to not be required for ferrous iron uptake (25). This conclusion was based on the absence of ferrous iron uptake defect in the *feoB* mutant of two strains of *C. jejuni*, M129 and F38011 (25). The genomes of these two strains have not been sequenced. Consequently, it is unknown whether these strains harbor an additional FeoB homolog or an alternative ferrous transport system, which could explain the observed phenotype of the *feoB* mutants. Given that the *feoB* mutant of *C. jejuni* NCTC 11168 was not tested in the present

* Corresponding author. Mailing address: Department of Biochemistry, Microbiology, and Immunology, Faculty of Medicine, University of Ottawa, 451 Smyth Road, Ottawa, Ontario K1H 8M5, Canada. Phone: (613) 562-5800, x8216. Fax: (613) 562-5452. E-mail: astintzi@uottawa.ca.

TABLE 1. Bacterial strains and plasmids used in this study

Strain or plasmid	Relevant characteristics or genotype[a]	Source
Strains		
E. coli		
DH5α	*endA1 hsdR17* (r_K^- m_K^-) *supE44 thi-1 recA1 gyrA relA1* Δ(*lacZYA-argF*)*U169 deoR* [ϕ 80*dlac*Δ(*lacZ*Δ M15)]	Invitrogen
C. jejuni		
AS144	*C. jejuni* NCTC 11168	NCTC
AS53	*C. jejuni* TGH9011 (ATCC 43431)	ATCC
AS275	*C. jejuni* 81-176	C. L. Pickett
AS217	AS144 *feoB*::Km^r	This study
AS236	AS53 *feoB*::Km^r	This study
AS237	AS275 *feoB*::Km^r	This study
Plasmids		
pILL600	Km^r resistance gene	A. Labigne
pCAP	Cloning and suicidal vector; Amp^r	Roche
pAS43	pCAP carrying *feoB*	This study
pAS223	pCAP carrying *feoB*::Km^r	This study

[a] Amp^r, ampicillin resistance gene.

TABLE 2. Primers used in this study

Primer	DNA sequence (5′–3′)
feo1	CGCTGGCCAAAGTCATTGATTTGCCAGGAAC
feo2	CGCTGGCCAGCCACTGCACTTGGTATAGG
Cj1395F	CGATTGCGATCCTTTAGAAGCAAA
Cj1395R	CGAGTGGTTTAAATTTTCTAGATTGATGA
Cj1397F	CGACGCTCACAAAGAACTCAAAAA
Cj1397R	CGAGCTTCATCAGATCTTAGGATAACACA
Cj1398F	CGATCAGCCTAATGTAGGCAAAAGTC
Cj1398R	CGATGCGTTCTAAATTGGTAGCATC
KmF	GATAAACCCAGCGAACCATT
KmR	TCTAGGTACTAAAACAATTCATCCAG
slyDR	GTCCATGTCCGTGATGATGA
slyDL	TGAAGCTTGATTGCCCTAGC
IlvCR	TGATCCAAGGCATCATAGCA
IlvCL	TAGGTGGTGGCACTCCTTGT

study and that its genome does not contain any other FeoB homolog, we reevaluated and further studied the function of FeoB in ferrous iron acquisition. Here, we present the role of FeoB in *C. jejuni* iron acquisition, gut colonization, and intracellular survival.

MATERIALS AND METHODS

Bacterial strains, plasmids, and growth conditions. The bacterial strains and plasmids used in the present study are listed in Table 1. *E. coli* DH5α was cultured aerobically at 37°C in Luria-Bertani (LB) broth or on LB agar plates. Plasmid containing strains were grown in a medium supplemented with ampicillin (100 μg/ml) or kanamycin (30 μg/ml). *C. jejuni* strains were routinely grown at 37°C in a MACS-VA500 microaerophilic workstation (Don Whitley, West Yorkshire, England) in an atmosphere of 83% N_2, 4% H_2, 8% O_2, and 5% CO_2 on Mueller-Hinton (MH) agar plates, MH broth medium, MH broth supplemented with 20 μM Desferal, or minimal essential medium (MEMα; Invitrogen) supplemented with 20 mM sodium pyruvate. Kanamycin was added as required at a concentration of 30 μg/ml. Prior to performing any in vitro cell culture studies or in vivo animal experiments, the *C. jejuni* strains were checked for motility on 0.4% MH agar plates.

Construction of *C. jejuni feoB* mutants. The *C. jejuni* NCTC 11168 chromosomal DNA was extracted by using the Wizard genomic DNA purification kit (Promega). An internal fragment of the *feoB* gene was PCR amplified by using the primers feo1 and feo2 (both containing a MluNI restriction site; Table 2). The resulting 1,617-bp PCR product was digested with MluNI and ligated to the MluNI-restricted pCAP vector to obtain pAS43 (pCAP-*feoB*). Then, the *feoB* gene was disrupted by insertion of a ClaI-restricted kanamycin-resistant (Km^r) cassette (which was excised from pILL600) in its unique ClaI site, yielding pAS223 (pCAP::*feoB*::Km). The orientation of the Km^r cassette was determined to be in the same direction as the *feoB* gene by PCR and restriction digestion. This final construct, pAS223, was used to transform *C. jejuni* NCTC 11168, 81-176, and ATCC 43431, using previously established protocols (20, 30). The *feoB* mutants were selected on MH agar plates containing 30 μg of kanamycin per ml, and the double homologous recombination event was confirmed by PCR using a combination of primers that amplified the Km^r (Table 2, primers KmF and KmR) and *feoB* genes (Table 2, primers feo1 and feo2).

RNA extraction and operon mapping by reverse transcription-PCR (RT-PCR). Total RNA was extracted from *C. jejuni* NCTC 11168 grown to mid-log-phase in iron-restricted MEMα using a hot phenol-chloroform protocol as previously described (20, 28, 30, 31). After ethanol precipitation, total RNA was suspended in RNase-free water and subjected to two successive DNase I (Invitrogen) treatments to remove any contaminating chromosomal DNA. Finally, RNA was further purified using an RNeasy kit (QIAGEN, Valencia, CA). The absence of genomic DNA was ensured by PCR using the feo1 and feo2 primers. The RNA integrity was confirmed by agarose gel electrophoresis, followed by quantification with RiboGreen RNA quantification reagent (Molecular Probes). The purified total RNA was stored at −80°C until further use.

The cotranscription of Cj1395, *feoA* (Cj1397), and *feoB* (Cj1398) was assessed by using 100 ng of DNase-treated total RNA and a combination of six primers (Table 2 and Fig. 1). First-strand cDNA synthesis and subsequent PCR amplification were performed by using the QIAGEN One-Step RT-PCR kit according to the manufacturer's recommendations and as previously described (20, 28, 30). The RT-PCR products were separated on 0.9% agarose gel with the 1-kb standard DNA ladder (Bayou-BioLabs).

Real-time quantitative RT-PCR. Real-time quantitative RT-PCR was performed by using the ABI Prism 7300 DNA analyzer (Applied Biosystems, Foster City, CA) and the QuantiTect SYBR green RT-PCR kit (QIAGEN) according to the manufacturer's protocol and as previously described (20, 28, 30, 31). Total RNA was extracted from *C. jejuni* wild-type and *feoB* mutant strains grown to mid-log phase in iron-restricted MEMα as described above for the operon mapping by RT-PCR. The relative expression level of the *feoA* gene in the wild-type and *feoB* mutant strains was normalized to either *slyD* (encoding the

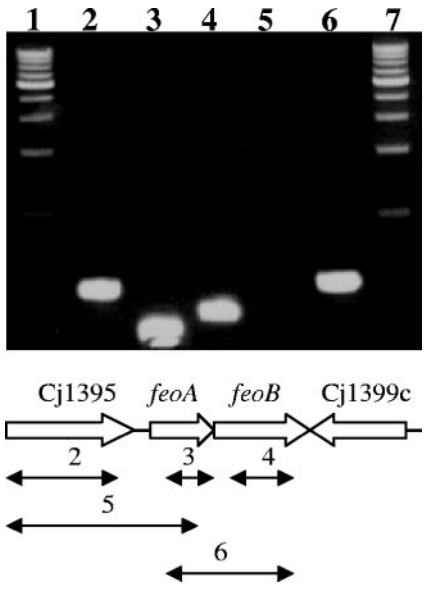

FIG. 1. Operon mapping by RT-PCR analysis. The predicted RT-PCR products within the Cj1395-to-Cj1399c genomic region are shown at the bottom. The RT-PCR product labels match the numbering of the agarose gel lanes. Lanes 1 and 7 correspond to the 1-kb ladder. The template RNA was extracted from *C. jejuni* NCTC 11168 cells grown in MEMα.

peptidyl-prolyl *cis-trans* isomerase) or *ilvC* (encoding the ketol-acid reductoisomerase). The expression of both *slyD* and *ilvC* was previously shown to be invariant to the iron content of the growth medium. The primers used are listed in Table 2. Quantitative values were obtained by using the comparative threshold cycle ($\Delta\Delta C_T$) method, as recommended by Applied Biosystems and as previously described (20, 28, 30, 31). The *feoA* transcript level from each RNA sample was assayed three times, and the mean C_T value was used for further analysis.

Ferrous iron uptake experiments. Wild-type and mutant strains of *C. jejuni* were grown to mid-log-phase under microaerophilic conditions in MH, MH-desferriferrioxamine (20 μM), or MEMα. The cells were centrifuged at 6,000 rpm for 15 min at 4°C, washed with 10 mM Tris buffer (pH 7.4), resuspended in the uptake buffer (5 g of Na_2HPO_4, 5 g of KH_2PO_4, 1.18 g of NH_4Cl, 0.089 g of Na_2SO_4, 0.042 g of $MgCl_2 \cdot 6H_2O$, and 10 g of Casamino Acids/liter) to an optical density at 600 nm (OD_{600}) of 0.6 (equivalent to 10^9 CFU/ml), and kept on ice. Then, 10 ml of the bacterial suspension was incubated at 37°C for 10 min, and ferrous iron transport assays were started with the addition of 0.037 μM $^{55}Fe^{2+}$. The $^{55}Fe^{2+}$ stock solution was prepared in the uptake buffer and contains 3.7 μM $^{55}FeCl_3$ (Perkin-Elmer, Boston, Mass.) and 60 mM sodium ascorbate to reduce iron. Samples of 1 ml were drawn at appropriate times, and the cells were immediately pelleted at 4°C by centrifugation at 13,000 rpm for 2 min. The pelleted cells were washed twice with 2 ml of 0.1 M citrate and resuspended in 500 μl of cold water. Incorporated iron was determined by liquid scintillation counting as previously described (29). The uptake assays were repeated at least three times, and the data were statistically analyzed by using the Student *t* test at a 5% level of significance.

Determination of cellular iron accumulation. *C. jejuni feoB* mutants and wild-type strains were grown in 25 ml of MEMα supplemented with 20 mM sodium pyruvate and 0.036 μM $^{55}Fe^{2+}$ (prepared as described above for the ferrous iron uptake experiments) at 37°C under microaerophilic conditions. Growth of the bacterial cultures was monitored by measuring the OD_{600}. The cellular accumulation of $^{55}Fe^{2+}$ was determined by drawing a 1-ml aliquot of the culture after 0, 8, 12, and 24 h of bacterial growth. The cells were centrifuged at 13,000 rpm for 2 min, washed twice with 0.1 M citrate, and resuspended in 500 μl of deionized water. Finally, the intracellular iron accumulation was determined by liquid scintillation counting as described above. The experiment was repeated three times and the data were statistically analyzed by using the Student *t* test at a 5% level of significance.

Determination of subcellular iron accumulation and localization. The iron content of the periplasmic space and cytoplasm after $^{55}Fe^{2+}$ uptake was determined by using the PeriPreps periplasting kit from Epicenter. At the appropriate time after the addition of $^{55}Fe^{2+}$, 1 ml of bacterial cells (OD_{600} = 0.6) was pelleted by centrifugation and washed twice with 0.1 M citrate. The cells were resuspended in 50 μl of PeriPreps periplasting buffer (200 mM Tris-HCl [pH 7.5], 20% sucrose, 1 mM EDTA and 30 U of Ready-Lyse lysozyme/μl) and incubated at room temperature for 5 min. Then, 50 μl of cold water was added to the bacterial suspension, followed by incubation for 5 min on ice to induce an osmotic shock. The resulting spheroplasts were centrifuged for 5 min at room temperature, and the supernatant containing the periplasmic fraction was transferred to a clean tube. The integrity of the spheroplasts was confirmed by electron microscopy. The pellet was washed twice with 0.1 M citrate and resuspended in 500 μl of cold water constituting the spheroplastic fraction. Finally, the $^{55}Fe^{2+}$ content of the periplasmic and spheroplastic fractions was determined by liquid scintillation counting. This experiment was repeated thrice and analyzed by using the Student *t* test at a 5% level of significance.

Invasion assay into INT-407 and IPEC-1 cells. Human INT-407 embryonic intestinal cells were obtained from the American Type Culture Collection and routinely maintained in MEMα, supplemented with 10% fetal bovine serum (Invitrogen). Porcine IPEC-1 small intestinal epithelial cells were obtained from H. M. Berschneider (North Carolina State University) and were routinely maintained on Dulbecco minimum essential medium (Invitrogen), supplemented with 5% fetal bovine serum (Invitrogen), insulin (5 μg/ml), transferrin (5 μg/ml), selenium (5 ng/ml) (Invitrogen), and epidermal growth factor (5 ng/ml; Invitrogen). Cells were grown in an incubator at 37°C under 5% CO_2.

The binding and invasion assays were carried out as previously described (24). Briefly, the binding assay was performed by coincubation of *C. jejuni* cells grown to mid-log phase in biphasic MH media with 24-h-grown, semiconfluent INT-407 cells or 48-h-grown IPEC-1 cells (~10^5 cells per well) at a multiplicity of infection of 10:1 (10 bacteria per eukaryotic cell). After 3 h of incubation at 37°C in the presence of 5% CO_2, the cell growth medium was removed, and the monolayer was washed thrice with Hanks balanced salt solution (HBSS). Thereafter, the infected cells were lysed with 0.1% Triton X-100 at room temperature for 30 min. Serial dilutions of the cell lysates were plated on MH agar plates to enumerate the number of bacteria bound to and internalized in the eukaryotic cells. For the invasion assay, the infected cells were incubated for an additional hour in fresh medium containing 250 μg of gentamicin per ml to kill the extracellular bacteria. Thereafter, the cells were washed three times with HBSS and lysed by using 0.1% Triton X-100 for 30 min at room temperature. The number of intracellular bacteria was determined by serial dilutions and enumeration on MH agar plates. The binding efficiency was obtained by subtracting the number of intracellular bacteria from the total number of bacteria recovered from cells not subjected to gentamicin treatment. The invasion efficiency was expressed as the percentage of inoculum recovered after gentamicin treatment. Each binding and invasion assay was repeated at least three times, and the data represent the means ± the standard errors. The data was statistically analyzed by using the Student *t* test at a 5% level of significance.

Determination of intracellular survival. The intracellular survival (ICS) assay was performed with semiconfluent INT-407 and IPEC-1 intestinal epithelial cells. After bacterial invasion and gentamicin treatment as described above for the binding and invasion assays, the eukaryotic cells were washed three times with HBSS and cultured for an additional 72 h in fresh MEMα supplemented with 10% fetal bovine serum. This medium was changed every 24 h. After the desired incubation time points (24, 48, and 72 h), and the monolayer was washed three times with HBSS and lysed with 0.1% Triton X-100 at room temperature for 30 min. The number of viable intracellular bacteria was determined by plating serial dilutions of the cell lysate suspensions on MH agar plates. The experiment was repeated three times, and the results shown are the mean ± the standard error. A Student *t* test was used for statistical analysis at a 5% level of significance.

Chick colonization model. One-day-old specific-pathogen-free chicks were obtained from Tyson Farms in Arkansas. On arrival, cloacal swabs of the chicks were taken to ensure that they were *Campylobacter* free. Housing was maintained at 25°C, and the chick cages were provided with a brooder which maintained a temperature in the range of 33 to 35°C. Chicks were given commercial chicken starter diet and water ad libitum. For challenge, *C. jejuni* wild-type and *feoB* mutant strains were grown in an MH biphasic medium. The bacteria were harvested at mid-log-phase and resuspended in phosphate-buffered saline (PBS) buffer. Each chick was inoculated (orally) with 0.25 ml of a bacterial suspension which contained ca. 10^4 to 10^5 viable bacteria. The bacterial titers of the inocula were confirmed by plating serial dilutions of the cultures on MH agar plates. The *feoB* mutant and wild-type strains of *C. jejuni* NCTC 11168, 81-176, and ATCC 43431 were separately inoculated into groups of five chicks. Five birds per group were inoculated separately with the wild-type or mutant strains. At 4 days postchallenge, the chicks were euthanized, the ceca were collected, and the contents were homogenized and checked for *C. jejuni* viable counts by plating serial dilutions on broth plates of *Campylobacter* agar base (Oxoid CM935) containing the *Campylobacter* selective Karmali antimicrobial supplements (Oxoid SR167E). Plates were incubated at 37°C for 72 h, and the bacterial recovery titer was determined and expressed as CFU per gram of ceca. A nonparametric Mann-Whitney rank sum test was used for statistical analysis at a 5% level of significance.

For the chick competitive colonization assays, each chick was inoculated with 0.5 ml of a bacterial suspension containing a 1:1 mixture of *C. jejuni* NCTC 11168 and its *feoB* mutant at 10^5 CFU/ml. The bacterial titer and the one-to-one ratio of the initial inoculum were confirmed by plating serial dilutions of the mixed culture on MH agar with or without kanamycin (30 μg/ml). At 4 days postinoculation, the chicks were euthanized, the ceca were collected, and their contents were homogenized, serially diluted in PBS buffer, and then plated onto *Campylobacter* selective agar plates, as described above, with or without kanamycin (30 μg/ml). The plates were then incubated at 37°C for 72 h in a microaerophilic chamber before the colonies were counted. The mutant titer was obtained from the CFU recovered on broth plates containing kanamycin, and the wild-type bacterial titer was calculated by subtracting the number of mutants from the total number of bacteria recovered on broth plates without kanamycin. Finally, the in vivo competitive index was calculated for each bird, which is the ratio of mutant to wild-type bacteria recovered (output ratio) divided by the ratio of mutant to wild-type bacteria inoculated (input ratio). The data were statistically analyzed by using a Student *t* test at a 5% level of significance.

Neonate piglet infectious model. Colostrum-deprived neonatal piglets were obtained from the swine farm of Oklahoma State University. The piglets were checked upon arrival with rectal swabs to verify that they were *Campylobacter* free. Piglets were group housed (segregated in experimental and control groups) in stainless steel swine pens with elevated vinyl coated floors. An ambient room temperature was maintained between 26 and 29°C with supplemental heat provided by one or more heat lamps to provide 32 to 35°C directly under the heat lamp(s). Room light timers were set to provide a 12-h dark/12-h light diurnal light cycle. Piglets were fed a milk replacer (Multi-Purpose milk replacer, Grade

A Ultra24; Sav-A-Caf Products) four times daily. This milk replacer was warmed to ca. 84 to 86°F prior to feeding. The initial feeding was within 60 min of birth. For the first day (24 h) piglets were either bottle-fed or fed using a 60-ml syringe. Subsequently, piglets were fed by placing milk replacer in shallow pans. Piglets were fed ca. 2 to 4 oz. (60 to 120 ml) per feeding. For the colonization assays, the 1- to 2-day-old piglets from the experimental groups were orally inoculated with a 20-ml mid-log-phase suspension of one of the three *C. jejuni* wild-type strains in Similac milk containing between 10^{10} and 10^{11} organisms per ml. Piglets were observed daily for clinical signs of disease (diarrhea, blood, and mucus in the stool) over a period of up to 3 days. The presence of blood in the feces was tested by using the EZ detection kit (Biomerica). Piglets were sacrificed at 3 days postinoculation. Any animal showing severe signs of debility (loss of strength, high fever, difficulty breathing, and/or no appetite), particularly if death appeared imminent, was immediately euthanized. Postmortem pathological changes of the gastrointestinal tract were recorded (e.g., hyperemia, edema, hemorrhage, or distention with gas). Immediately after euthanasia, necropsy was performed, and the duodenum, jejunum, ileum, colon, and cecum were independently excised and processed for histopathological analysis and *C. jejuni* enumeration as previously described (30).

For the in vivo competition assay, each *feoB* mutant and its wild-type strain were mixed at a one-to-one ratio (~5×10^{10} CFU per strain). The titer of the mutant and wild-type was determined, and the competitive index was computed and statistically analyzed as described earlier for the chick competitive colonization assay.

RIL model. The in vivo competitive index of the *feoB* mutant and the wild-type NCTC 11168 in the rabbit ileal loop (RIL) model was determined as previously described (30). Briefly, two New Zealand White rabbits (<2 kg; female) were anesthetized, a laparotomy was performed, and two 20-cm sections of ileum with intact mesenteric blood supply were ligated per animal. The four ileal loops (from two rabbits) were each injected with a 1-ml PBS suspension of a 1:1 mixed culture containing ca. 10^6 CFU (each) of *C. jejuni* NCTC 11168 wild-type and *feoB* mutant strains/ml. The 1:1 mixed inocula of the mutant and wild-type strains were confirmed by plating serial dilutions of this mixed culture on MH agar with or without kanamycin (30 μg/ml). The loops of two additional rabbits were inoculated with sterile PBS buffer and served as uninfected controls. After inoculation, the exteriorized intestinal loops were repositioned in the abdominal cavity, and the abdominal wall and skin were finally closed as per standard procedures. At 48 h postinoculation, the rabbits were anesthetized again, the intestinal loops were excised intact, and the animals were euthanized. The contents of the loops (including the mucous layer) were homogenized in 10 ml of PBS buffer and serial diluted. The titers of the *feoB* mutants and the wild-type strains were determined as described above for the chick and piglet animal models. Finally, the in vivo competition index for each loop was calculated, and the data were statistically analyzed by using the Student *t* test at a 5% level of significance.

RESULTS

Sequence analysis, operon mapping, and mutation of *C. jejuni feoB*. The analysis of the *C. jejuni* NCTC 11168 genome reveals the presence of two genes, Cj1397 and *feoB*, whose products share significant identities at the amino acid level with the *E. coli* FeoA (16%) and FeoB (29.3%) proteins, respectively (21). The *C. jejuni* FeoB protein has 50.5% identity with the *H. pylori* FeoB and is predicted to be an integral cytoplasmic protein of 613 amino acids, containing 10 potential transmembrane α-helices and an ATP/GTP binding site at the N-terminal region. Cj1397 is predicted to encode a protein similar in size to the *E. coli* FeoA (77 amino acids) and contains the FeoA conserved protein domain as shown by RPS-BLAST analysis (17). The *feoA* and *feoB* genes appear to be in an operonic structure and are divergently transcribed from Cj1399c (Fig. 1), which encodes a probable Ni/Fe-hydrogenase small subunit. The open reading frame upstream of *feoA*, Cj1395, is a pseudogene which encodes an hypothetical protein of unknown function. In order to experimentally demonstrate the cotranscription of *feoA* (Cj1397) and *feoB* genes, we performed RT-PCRs with primers that anneal within and across pairs of the Cj1395, *feoA*, and *feoB* genes (Fig. 1). Each RT-PCR gave a product of the expected size, demonstrating the operonic structure of the *feoA* (Cj1397) and *feoB* genes.

To determine the function of FeoB in the *C. jejuni* ferrous iron acquisition, we constructed a *feoB* mutant by marker exchange mutagenesis (see Materials and Methods) into three strains of *C. jejuni*, the genome sequenced strain *C. jejuni* NCTC 11168, and the two clinical isolates *C. jejuni* 81-176 and *C. jejuni* ATCC 43431. Analysis of the recently released genome information of *C. jejuni* 81-176 at the NCBI database reveals the presence of the *feoA-feoB* operon with the same genetic organization as in *C. jejuni* NCTC 11168. Although the genome of *C. jejuni* ATCC 43431 has not been sequenced, we have recently characterized its gene content by DNA and shotgun microarray analysis. This study indicated the presence of both *feoA* and *feoB* genes (23, 24).

We have been unable to complement the *feoB* mutants using the shuttle vector pRY112. Consequently, to confirm that the *feoB* mutation was nonpolar, the level of expression of *feoA* was quantified by real-time RT-PCR in the three wild-type strains and *feoB* mutants. To note, the gene downstream of *feoB*, Cj1399, is divergently transcribed from *feoB* in both *C. jejuni* NCTC 111168 and 81-176 strains (Fig. 1), and thus its expression level will not be affected by the mutation. The genetic organization of the *feoAB* operon in *C. jejuni* ATCC 43431 is unknown. Consequently, we could not assert whether the expression of the gene downstream of *feoB* will be affected by the *feoB* mutation in *C. jejuni* ATCC 43431. The expression level of the *feoA* gene was found to be increased in the *feoB* mutants (six- to eightfold) compared to their wild-type strains. This result indicates that the insertion of the kanamycin cassette into the *feoB* gene does not destabilize the *feoAB* transcript. Consequently, the mutation is nonpolar. In addition, the increase of the *feoA* expression level in the *feoB* mutants suggests that the *feoAB* operon expression is tightly regulated.

Uptake of ferrous iron. In order to assess the role of FeoB in ferrous iron acquisition, we compared the capacity of the wild-type and *feoB* mutant of *C. jejuni* NCTC 11168 to uptake ferrous iron (Fig. 2). The ^{55}Fe iron uptake assay was performed in the presence of sodium ascorbate in order to maintain the ferrous reduction state and using *C. jejuni* cells grown to mid-log phase in iron-restricted medium (MH broth supplemented with 20 μM Desferal as previously described [20]). As shown in Fig. 2, the *C. jejuni* NCTC 11168 cells accumulate up to 7.5 pmol of ferrous iron per OD_{600} upon 15 min incubation with $^{55}Fe^{2+}$. In contrast, the *feoB* mutant cells are significantly affected and incorporate only 0.8 pmol of ferrous iron per OD_{600} over the assay period ($P < 0.05$). This 10-fold decrease in ferrous iron accumulation indicates that FeoB has a critical role in iron acquisition.

Because the FeoB protein is predicted to be an integral protein involved in the transport of ferrous iron across the cytoplasmic membrane, the iron accumulated by the *feoB* mutant could be solely localized in the periplasmic space. To investigate the cellular localization of ferrous iron upon incubation with $^{55}Fe^{2+}$, the bacterial cells were osmotically shocked (using the PeriPreps periplasting kit from Epicenter) and the periplasmic and cytosolic fractions were collected. Exposure of gram-negative bacteria to osmotic shock has been previously shown to result in the formation of spheroplasts and

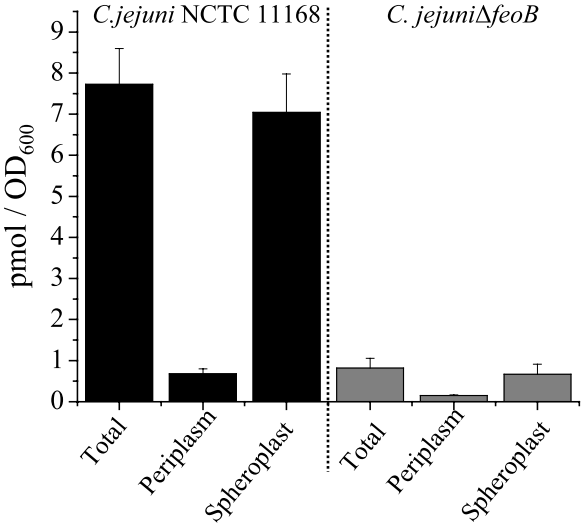

FIG. 2. Uptake of $^{55}Fe^{2+}$ by *C. jejuni* NCTC 11168 and its *feoB* mutant. Cells grown to mid-log phase in iron-restricted medium (MH medium supplemented with 20 μM Desferal) were incubated with 0.036 μM $^{55}Fe^{2+}$ for 15 min in the presence of 0.6 mM sodium ascorbate. The columns represent the iron accumulation in the whole cells (total), the periplasmic space (periplasm), and the cytosol (spheroplast) of the wild-type strain (■) and the *feoB* mutant (▨). The data are representative of two independent experiments. Error bars indicate the standard deviation.

the substantial release of proteins and solutes from the periplasmic space (5). The formation of *C. jejuni* spheroplasts was confirmed by electron microscopy (data not shown). Although the electron microscopy could not assert the complete absence of cytosolic release, it did confirm the formation of significant breaks into the outer membrane, indicating that periplasmic solutes would be discharged upon such treatment. Figure 2 shows that up to 90% of the transported iron accumulates within the cytosol of both the wild-type and the *feoB* mutant strains. This result indicates that the iron accumulated by the *feoB* mutant under these conditions is not blocked into the periplasmic space but is still transported into the cytoplasm via a non-FeoB-dependent mechanism.

Growth characteristics and accumulation of iron. To determine whether ferrous iron acquisition plays an important role in the growth of *C. jejuni*, we compared the ability of *C. jejuni* NCTC 11168 wild-type and *feoB* mutant strains to grow in MEMα with or without added ferrous iron at a 0.036 μM final concentration. While the MEMα contains trace amount of iron, it has been previously used by us and others as an iron-limited growth medium (20, 34). The growth yield of the *feoB* mutant is slightly lower than the wild-type strain in MEMα with or without added ferrous iron (Fig. 3A, closed and open symbols, respectively), suggesting that the FeoB protein promotes bacterial growth. Interestingly, the addition of 0.036 μM ferrous iron to the MEMα stimulates the growth of the wild-type strain only. This observation is in agreement with the role of FeoB as a major route for ferrous iron acquisition.

To monitor cellular iron accumulation, the wild-type and *feoB* mutant strains were grown in MEMα supplemented with 0.036 μM $^{55}Fe^{2+}$, and the levels of intracellular iron were quantitatively determined at various time points during growth

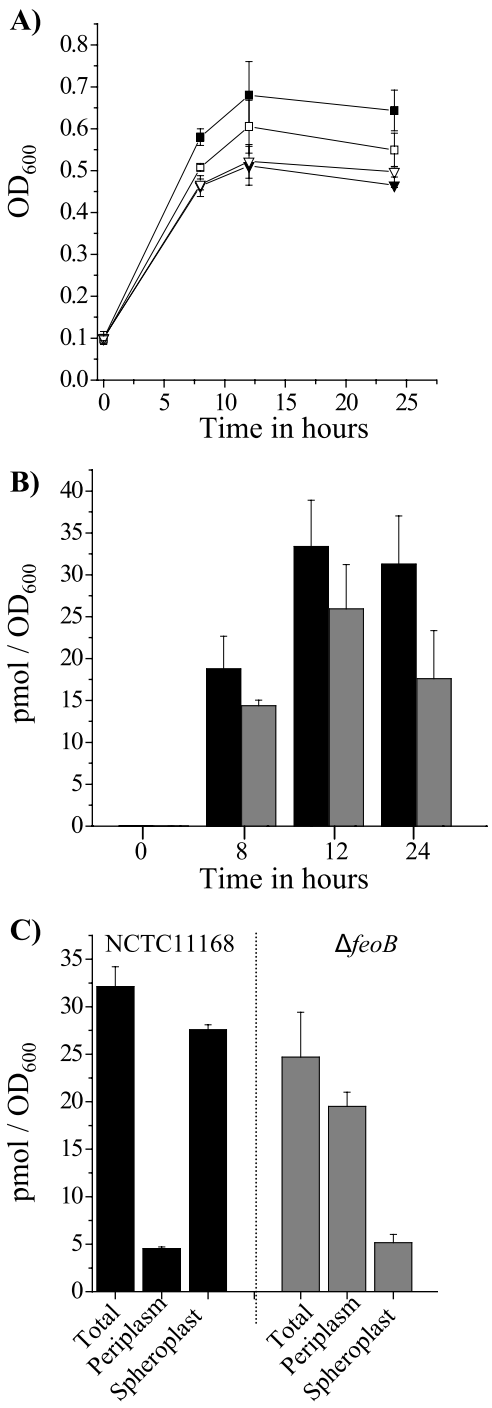

FIG. 3. Amount of Fe^{2+} taken up by the wild-type *C. jejuni* NCTC 11168 and its *feoB* mutant during growth. (A) Growth of *C. jejuni* NCTC 11168 (squares) and its *feoB* mutant (inverted triangles) in iron limited MEMα plus 20 mM sodium pyruvate (open symbols) or in MEMα plus 20 mM sodium pyruvate supplemented with 0.036 μM $^{55}Fe^{2+}$ (closed symbols) and 0.6 mM sodium ascorbate. (B) Accumulation of $^{55}Fe^{2+}$ in *C. jejuni* NCTC 11168 (■) and its *feoB* mutant (▨) grown in medium MEMα plus 20 mM sodium pyruvate plus 0.036 μM $^{55}Fe^{2+}$ at 0, 8, 12, and 24 h of growth. (C) Iron accumulation in the whole cells (total), in the periplasmic space (periplasm) and in the cytosol (spheroplast) of the wild-type strain (■) and the *feoB* mutant (▨) grown for 12 h in MEMα plus 20 mM sodium pyruvate plus 0.036 μM $^{55}Fe^{2+}$. Each datum point represents the mean of at least two independent experiments. Error bars indicate the standard deviations.

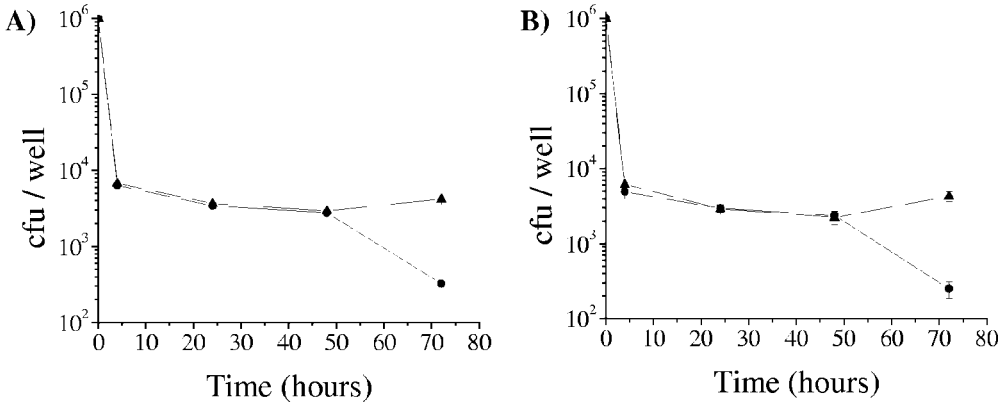

FIG. 4. Invasion and intracellular survival of *C. jejuni* 81-176 (▲) and its *feoB* mutant (●) in human INT-407 embryonic intestinal cells (A) and in porcine IPEC-1 small intestinal epithelial cells (B). Epithelial cells were infected with the wild-type strain and *feoB* mutant at a multiplicity of infection of 10:1 (number of bacteria per eukaryotic cell), and the survival kinetics were analyzed over a 72-h period. *Campylobacter* cells were grown in MH medium before infection. The first datum point at time zero hour represents the bacterial inoculum (10^6 bacteria). The experiment was repeated thrice and the data represent the mean ± the standard error.

by liquid scintillation counting. As shown in Fig. 3B, the *feoB* mutant accumulates, at the stationary phase, the labeled ferrous iron to an extent of 1.5-fold lower than the wild-type strain. Interestingly, the analysis of intracellular iron localization (as described above) indicates that the iron accumulated in the *feoB* mutant is essentially localized in the periplasmic space (80% of the total accumulated iron; Fig. 3C). In contrast, the wild-type strain accumulates 87% of its iron content into its cytosol (Fig. 3C). To note, iron accumulation in the periplasmic space of the *feoB* mutant was not observed during the iron uptake experiment (Fig. 2) likely as a result of the short 15-min incubation time with labeled ferrous iron under this experimental setting. In fact, the total amount of labeled iron accumulated in the *feoB* mutant is 30-fold lower during the uptake experiment compared to the accumulation assay. Altogether, these data indicate that *C. jejuni* FeoB is the major route for the transport of ferrous iron across the cytoplasmic membrane. This conclusion is in agreement with the annotation of FeoB as an integral membrane protein.

Intracellular survival of the *C. jejuni feoB* mutant in INT-407 and IPEC-1 cells. To understand the contribution of ferrous iron acquisition for survival in eukaryotic cells, we tested the ability of the *C. jejuni feoB* mutant to survive intracellularly up to 72 h. Given the low efficiency of *C. jejuni* NCTC 11168 to invade eukaryotic cells (24), these assays were performed with the wild-type and *feoB* mutant strains of *C. jejuni* 81-176, previously shown to have a high invasion efficiency (23).

Human INT-407 embryonic intestinal cells and porcine IPEC-1 small intestinal epithelial cells were infected with the wild-type and *feoB* mutant strains at a multiplicity of infection of 10 to 1 for 3 h, and the survival kinetics were analyzed over 72 h (Fig. 4). The integrity of the cell monolayers was maintained by changing the growth medium every 24 h and was checked under an inverted microscope. The wild-type and *feoB* mutant strains exhibit similar invasion efficiencies with ca. 0.6% of the inocula invading the intestinal cells. The binding efficiencies were also indistinguishable between both strains (data not shown). As illustrated in Fig. 4, both strains exhibit similar survival characteristics during the first 48 h. At 72 h postinfection, the *feoB* mutant is significantly affected in its ability to persist within INT-407 and IPEC-1 cells ($P < 0.05$). It is approximately five- and eightfold more sensitive than the wild-type strain in its ability to survive within IPEC-1 and INT-407 cells, respectively (Fig. 4A and B). These data indicate that FeoB plays an essential role in *C. jejuni* intracellular survival. Consequently, ferrous iron might constitute an important iron source in the eukaryotic intracellular environment.

Colonization of the chick cecum. To examine the role of FeoB in *C. jejuni* colonization, the wild-type and *feoB* mutant strains of *C. jejuni* NCTC 11168, 81-176, and ATCC 43431 were tested in the chick animal model of colonization as previously described (20). Each mutant and wild-type strain was orally administered to five birds at a dose between 10^4 and 10^5 viable bacteria, and the level of bacterial colonization in the chick cecum was evaluated 4 days postinoculation by plate counting. To note, the isolate of *C. jejuni* 81-176 used in the present study is a relatively poor colonizer of the chick cecum compared to the two other strains, since it colonizes the cecum at a level of approximately 10^5 CFU per g compared to $\sim 5 \times 10^7$ for the two other strains of *C. jejuni* (Fig. 5). As shown in Fig. 5, the three *feoB* mutants are significantly affected in their ability to colonize the chick cecum compared to their respective wild-type strains ($P < 0.05$, using a nonparametric Mann-Whitney rank sum test). These data indicate that FeoB significantly promotes *C. jejuni* colonization of the chick cecum.

Interestingly, the *feoB* mutants of *C. jejuni* 81-176 appear to be less affected than the *feoB* mutants of *C. jejuni* NCTC 11168 and ATCC 43431 in its ability to colonize the chick cecum (Fig. 5). The *feoB* mutants of *C. jejuni* ATCC 43431, NCTC 11168, and 81-176 showed approximately (5×10^4)-fold, (2×10^4)-fold, and 31-fold decreases in their colonization ability compared to their corresponding wild-type strains, respectively. This observation suggests that *C. jejuni* strains differ in their requirement for iron and/or their capacity to acquire iron in vivo.

Colonization of the rabbit ileal loop. We have recently shown by genome-wide expression profiling that the *C. jejuni* NCTC 11168 *feoB* gene is expressed in vivo during host colo-

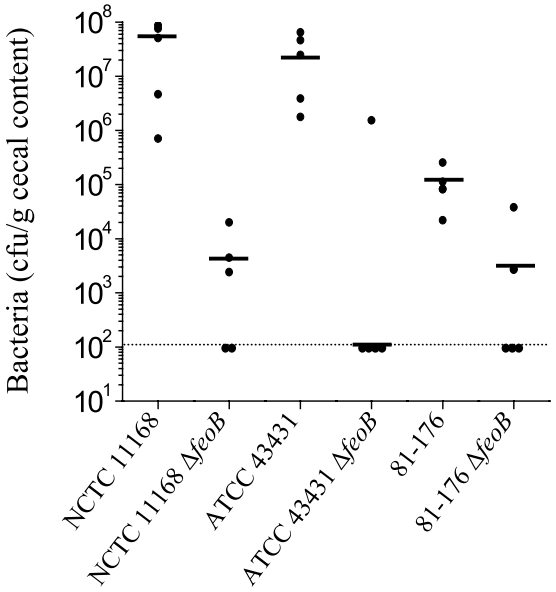

FIG. 5. Colonization of the chick cecum by *C. jejuni* wild-type strains NCTC 11168, 81-176, and ATCC 43431 and their derivative *feoB* mutants. Sets of five chicks were fed 10^4 to 10^5 cells of one of the wild-type strains *C. jejuni* or their derivative *feoB* mutants. At 5 days postinoculation the ceca were recovered, homogenized, serial diluted, and plated on selective medium for *C. jejuni* enumeration as previously described. Each point represents the colonization level (in CFU per gram of cecum) of each strain from a single chick. The dash line indicates the limit of detection, and the bars indicate the median bacterial colonization level.

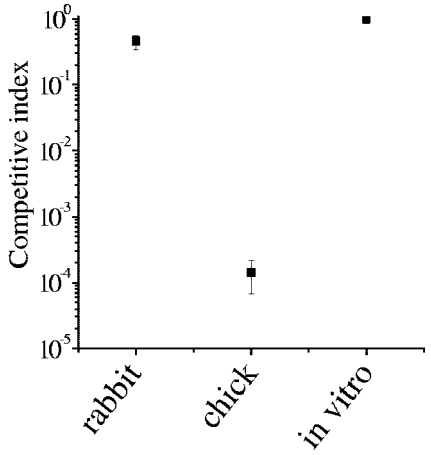

FIG. 6. Competitive index analysis of *C. jejuni* NCTC 11168 and its *feoB* mutant in the rabbit ileal loop, in the chick cecum, and in vitro. For the rabbit competition assay, the *feoB* mutant was mixed with the wild-type strain at a ratio of 1 to 1 and inoculated into four ileal loops. The rabbit competitive index is the ratio of the mutant to the wild-type strain recovered at 48 h postinoculation. For the chick colonization assay, five chicks were inoculated with a mixture of the *feoB* mutant and wild-type strain at a ratio of 1 to 1. The chick competitive index is the ratio of the mutant to the wild-type strain recovered 5 days postinoculation. The in vitro competitive index is the ratio of the *feoB* mutant and wild-type strain in MH broth at early stationary phase. A competitive index of 1 indicates that the *feoB* mutant is not affected. The data represent the means ± the standard errors.

nization using the rabbit ileal loop model (30). Consequently, in order to further study the mechanism of *C. jejuni* NCTC 11168 iron acquisition in the intestinal tract of rabbit, we tested the ability of the *feoB* mutant to colonize the rabbit ileal loop relative to the wild-type strain in a competition assay. The *feoB* mutant and the wild-type strains were pooled together at a 1-to-1 ratio and inoculated into four ileal loops constructed in two different rabbits. After 48 h postinoculation, the ileal loops were recovered and processed for bacterial enumeration by plating the loop contents on selective media. Then, the in vivo competitive index was calculated by dividing the number of *feoB* mutant strains recovered by the number of wild-type strains recovered. Similarly, we determined the in vitro competitive index at the stationary phase by inoculating MH broth with an equal amount of the wild-type and the *feoB* mutant strains (the in vitro experiment was performed in triplicate). As shown in Fig. 6, the *feoB* mutant exhibits an in vivo and in vitro competitive index of 0.46 ± 0.11 and 1.00 ± 0.05, respectively. This 2.2-fold difference was found to be statistically significant using a Student *t* test ($P < 0.01$). These data indicate a slight growth and/or survival defect of the *feoB* mutant in the rabbit ileal loop.

In order to directly compare the colonization ability of the *feoB* mutant in the rabbit ileal loop and chick models, we determined the competitive index of the *feoB* mutant in the chick model. The competitive index of the *feoB* mutant in this animal model is $(1.4 \times 10^{-4}) \pm (7.3 \times 10^{-5})$ (Fig. 6), which is significantly lower than in the rabbit ileal loop model ($P < 0.0001$). This difference in the competitive indices likely reflects the presence of more severe bottlenecks in the chick competitive colonization assay versus the rabbit ileal loop model. In the rabbit ileal loop model, once the *feoB* mutant and the wild-type strains are introduced in the intestinal loop, they will have to compete essentially only for growth nutrients and survival under these conditions. In contrast, in the chick competitive colonization assay, the mutant and wild-type strains will have to survive the exposure to the low pH of the gizzard, establish a colonization of the gut, compete for nutrients, and survive under more stressful conditions. The presence of bottlenecks in the chick colonization process has been described by others (10) and likely accounts for the difference in the competitive indexes observed in our two colonization assays.

Colonization of the piglet intestine. To investigate whether the *C. jejuni feoB* mutant was defective in colonization in an animal model that mimics human infection, competition assays were performed in the newborn piglet model for campylobacteriosis (2).

Given that the level of *C. jejuni* colonization in this animal model has never been reported, we tested the ability of the three strains of *C. jejuni* used in the present study to colonize the gastrointestinal tract of newborn piglets and to induce the development of diarrhea and clinical signs of disease. Groups of three newborn colostrum-deprived piglets were orally challenged with a bacterial suspension of either *C. jejuni* NCTC 11168, 81-176, or ATCC 43431 at a dose of ca. 5×10^{10} viable bacteria. An additional group of three noninfected piglets was kept as control. In contrast to the method described by Babakhani et al. (2), the piglets were fed a multipurpose milk replacer (Sav-A-Caf) instead of Similac (Ross Laboratories,

TABLE 3. Piglet infectious model

Site	Control	Mean CFU/g of tissue (SD) for *C. jejuni* strain[a]:		
		NCTC 11168	ATCC 43431	81-176
Duodenum	ND[b]	3.2×10^5 (2.5×10^5)	1.1×10^3 (1.2×10^2)	1.8×10^4 (1.0×10^4)
Jejunum	ND	6.2×10^4 (4.5×10^4)	1.2×10^5 (1.0×10^5)	2.8×10^4 (1.0×10^4)
Ileum	ND	9.3×10^4 (4.6×10^4)	4.2×10^5 (3.9×10^4)	2.0×10^4 (8.4×10^3)
Cecum	ND	1.5×10^7 (9.1×10^6)	2.1×10^4 (1.7×10^4)	7.1×10^3 (2.8×10^3)
Colon	ND	2.8×10^6 (1.3×10^6)	1.7×10^3 (7.7×10^2)	1.2×10^5 (6.3×10^4)
Diarrhea	Absent	Present	Present	Present
Blood in feces[c]	Absent	Absent	Present	Present

[a] Three colostrum-deprived piglets were infected orally with approximately 5×10^{10} viable bacteria of each *C. jejuni* strain. At 3 days postinfection, the piglets were euthanized, and the level of bacterial colonization was determined for each intestinal segment (duodenum, jejunum, ileum, cecum, and colon). The data represent the mean CFU for each strain per gram of tissue.
[b] ND, *C. jejuni* was not detected in the control piglets.
[c] The presence of blood in the feces was tested using the EZ detection kit.

Columbus, Ohio), because in the course of pilot studies we have noticed that Similac feeding induces the development of soft feces and protein deficiency. Piglets were observed for clinical signs of disease over a period of 3 days. The piglets infected with the strains of *C. jejuni* developed diarrhea 12 to 24 h postinoculation (Table 3). No diarrhea was observed in the piglets from the control group. Interestingly, the presence of blood was solely identified in the loose feces of animals infected with *C. jejuni* ATCC 43431 and 81-176 and not those infected with *C. jejuni* NCTC 11168 (Table 3). After 3 days of infection, most of the infected piglets showed signs of debility precluding the extension of this animal experiment beyond 3 to 4 days of infection. Consequently, the piglets were euthanized at 3 days postinfection and the duodenum, jejunum, ileum, cecum, and colon sections of the gastrointestinal tract were recovered. Then, each section was processed for histopathological analysis and *C. jejuni* enumeration on selective medium. As shown in Table 3, *C. jejuni* colonizes the piglet gastrointestinal tract at a level ranging from 10^3 to 10^7 CFU per g of intestinal content. The level of *C. jejuni* colonization varies along the gastrointestinal tract and is different between the three strains of *C. jejuni* (Table 3). For instance, *C. jejuni* NCTC 11168 colonizes the cecum at a level of 1.5×10^7 CFU/g, while *C. jejuni* 81-176 and ATCC 43431 colonize the same intestinal section only at levels of 7.1×10^3 and 2.1×10^4 CFU/g, respectively. Histopathological analysis of the intestinal sections did not reveal the presence of severe pathological lesions at 3 days postinfection. This is in agreement with the previous report from Babakhani et al., who observed significant lesions only after 6 days of infection (2). Nevertheless, the excretion of loose feces and the presence of blood in the feces of piglets infected with *C. jejuni* 81-176 and ATCC 43431 indicate that this animal model mimics human infection.

Finally, the capacities of the *feoB* mutants to compete with their respective wild-type strain for colonization and survival in the piglet gastrointestinal tract were determined by a competition assay. The competitive index was determined (as described earlier) for each strain of *C. jejuni* in vitro and for each section of the piglet gastrointestinal tract (duodenum, jejunum, ileum, cecum, and colon). The *feoB* mutants were found to be unaffected in vitro (in MH broth) with a competitive index equal to 1.00 ± 0.05. As shown in Fig. 7, the *feoB* mutants of *C. jejuni* NCTC 1168, ATCC 43431, and 81-176 are significantly affected in their abilities to colonize the piglet intestine ($P < 0.0001$). The *feoB* mutant of *C. jejuni* ATCC 43431 is the most affected mutant, followed by the *feoB* mutant of *C. jejuni* 81-176 and then the *feoB* mutant of *C. jejuni* NCTC 11168. This difference in growth defect between the three *feoB* mutants indicates that the three strains of *C. jejuni* should significantly differ in their growth requirement for iron and/or their capacities, other than FeoB-mediated, to acquire iron. Interestingly, the colonization defect of the *feoB* mutant of *C. jejuni* ATCC 43431 varies within the gastrointestinal tract. The number of *C. jejuni* ATCC 43431 *feoB* mutant was below the detection limit in the duodenum, jejunum, ileum, and colon sections (<100 CFU/g). However, the *feoB* mutant of *C. jejuni* ATCC 43431 was recovered from the cecum, albeit at a much lower level than the wild-type strain (with a competitive index of 0.035 ± 0.030). These data indicate the presence of different iron sources and/or differential bacterial iron requirement within the gastrointestinal tract. Altogether, these in vivo competitive assays highlight a major role for FeoB in piglet gut colonization.

DISCUSSION

Bacterial colonization of the host gastrointestinal tract depends in part on the ability of the bacteria to acquire essential growth nutrients. Iron is known to be a vital element for almost all living microorganisms (1). However, little is known about the bioavailability and sources of iron for enteric microbes in the gastrointestinal niche. Most of the iron that enters the intestine in the diet is in the oxidized ferric form. While the low-oxygen tension in the intestine will likely favor the reduction of iron to ferrous iron Fe^{2+}, the level of ferrous iron in this environment is unknown. The role of ferrous iron acquisition in gut colonization is poorly studied. However, genome sequencing projects reveal that most enteric gram-negative bacteria are equipped with a Fe^{2+} active transport system named Feo (1, 11). In addition, *feoB* mutants of *S. enterica* serovar Typhimurium, *H. pylori*, and *E. coli* have been shown to exhibit significant intestinal colonization defects (32, 33, 35). Altogether, these data indicate that ferrous iron might constitute an important iron source of the intestinal environment. Given that *C. jejuni* primarily resides within the host intestine, we

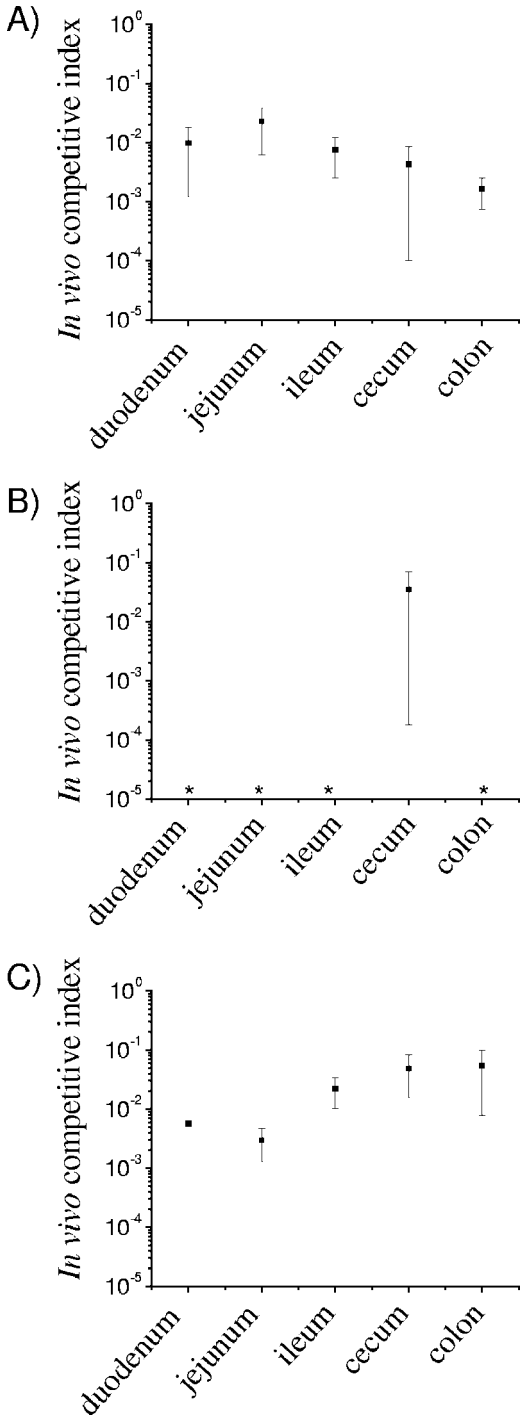

FIG. 7. Competitive index analysis of the wild-type strains *C. jejuni* NCTC 11168 (A), ATCC 43431 (B), and 81-176 (C) and their respective *feoB* mutant in the gastrointestinal tract of piglets. Each wild-type strain and its *feoB* mutant were mixed at a ratio of 1 to 1 and inoculated into three piglets. At 72 h postinoculation, the piglets were euthanized, and the intestinal segments (duodenum, jejunum, ileum, cecum, and colon) were collected. The competitive index was calculated as the ratio of the output mutant to the wild-type strain recovered divided by the ratio of the input mutant to the wild-type strain inoculated. The data represent the means ± the standard errors. An asterisk indicates that the number of *feoB* mutant per gram of intestine was below the detection limit of our assay (100 CFU/g), and consequently a competitive index was not calculated.

proposed to characterize its Fe^{2+} transport system and address its importance for gut colonization.

The analysis of the *C. jejuni* NCTC 11168 genome reveals the presence of a single potential FeoAB Fe^{2+} transporter system (21). In this report we provide many evidences that *C. jejuni* FeoB is part of a functional ferrous iron transporter system. First, *C. jejuni* NCTC 11168 FeoB is highly homologous to the *E. coli* and *H. pylori* FeoB proteins. Second, a *feoB* mutant of *C. jejuni* is significantly affected in its ability to transport ferrous iron (Fig. 2; $P < 0.05$). Third, the *C. jejuni feoB* mutant accumulates a lower amount of iron during growth compared to the wild-type strain (Fig. 3). Finally, the intracellular iron accumulated by the *feoB* mutant is localized in the periplasmic space compared to the cytosol for the wild-type strain (Fig. 3C), a result that is in agreement with the function of FeoB as a cytoplasmic membrane transporter.

Notably, our functional characterization of FeoB is in disagreement with the recent report from Raphael and Joens that indicates that FeoB is not required for ferrous iron uptake in *C. jejuni* (25). Raphael and Joens drew their conclusion from the absence of Fe^{2+} uptake defect in the *feoB* mutants of *C. jejuni* M129 and F38011 (25). In contrast, we characterized the function of FeoB by constructing an *feoB* mutant into the well-defined genome sequenced strain of *C. jejuni* NCTC 11168, which is known to harbor a single *feoB* homolog. Given that the genomes of *C. jejuni* M129 and F38011 have not been sequenced, these two strains might possess an alternative ferrous iron transporter, explaining the observations from Raphael and Joens (25). Alternatively, the absence of observable ferrous iron uptake defect in the *feoB* mutant from Raphael and Joens could be the result of their experimental approach (25). In that report, the *C. jejuni* cells used to perform the ferrous iron uptake assay were grown on MH plates, an iron-containing growth medium (25). In contrast, we grew *C. jejuni* in iron-limited MEMα. Although the regulation of the *feoB* expression in *C. jejuni* is unknown, the ferrous iron uptake system of other bacteria has been shown to be repressed by iron. Consequently, the FeoB-mediated ferrous iron transport is unlikely to be functional in iron-loaded cells, as would be *C. jejuni* cells grown on MH plates. In order to test this possibility and address the results from Raphael and Joens (25), we compared the capacity of the wild type and *feoB* mutant of *C. jejuni* NCTC 11168 to transport ferrous iron by using cells grown on MH plates (data not shown). The *feoB* mutant of *C. jejuni* NCTC 11168 exhibited no defect in ferrous iron uptake under such growth conditions (data not shown), which is in agreement with the phenotype of the *feoB* mutants of *C. jejuni* M129 and F38011 (25). In summary, our data clearly demonstrate the role of FeoB in ferrous iron uptake in *C. jejuni* under iron-limited conditions and suggest that the FeoB transporter system might be iron regulated. The regulation of the *feoB* gene is currently under investigation.

The importance of ferrous iron acquisition for bacterial intracellular survival and growth is evinced by several examples. The *feoB* mutant of *Legionella pneumophila* exhibits impaired replication in amoeba and human U937 cell macrophages, highlighting an important role for the FeoB system in intracellular infection (26). While mutants of *Shigella flexneri* defective in a single iron transporter system—*feoB*, *sitA* (which encodes a component of an iron transporter system), or *iucC* (which

encodes a component of the aerobactin transporter system)—show no defect in intracellular growth, double mutations in the *feoB* gene and any one of the two other transporter systems (*sitA* or *iucC*) significantly decrease the capacity of *S. flexneri* to form plaque on Henle cell monolayers (27). These findings indicate that both ferrous and ferric iron acquisitions contribute to the intracellular replication of *S. flexneri* (27). Likewise, only the double mutant in *feoB* and *sitA* of *S. enterica* serovar Typhimurium was impaired in its ability to replicate intracellularly (4). Based on these observations, the ferrous iron appears to be an important intracellular iron source for pathogens. Similarly, our data indicate that FeoB-mediated Fe^{2+} uptake is required for *C. jejuni* survival within human INT-407 embryonic intestinal cells and porcine IPEC-1 small intestinal epithelial cells. Although the intracellular persistence of the *feoB* mutant is similar to the wild-type strain during the first 48 h, it is inhibited for survival by approximately five- or eightfold at 72 h, depending on the cell lines (Fig. 4). This observation indicates that the amount of iron stored by the *feoB* mutant might be sufficient to persist within epithelial cells over the course of a 48-h incubation time and that the acquisition of iron via the FeoB system is only required for persistence past this initial stage. These findings add the *feoB* gene to the list of three other genes known to encode proteins contributing to intraepithelial or intramacrophage cell survival. These genes are *spoT* encoding a bifunctional (p)ppGpp synthetase/hydrolase (9), *katA* encoding a catalase (7), and *sodB* encoding a superoxide dismutase (22). Cellular invasion and intracellular survival have been associated with *C. jejuni* virulence (13). Indeed, mutants affected in their invasion ability were also shown to exhibit reduced virulence in the ferret animal disease model (3). Consequently, the *C. jejuni feoB* mutant, in addition to its colonization defect, might have attenuated virulence potential.

We have recently shown the expression of the *C. jejuni feoB* gene in rabbit ileal loops, suggesting an important role for FeoB in *Campylobacter* gut colonization and/or survival (30). To address this hypothesis, we compared here the ability of the *feoB* mutant and *C. jejuni* NCTC 11168 wild-type strain to colonize the rabbit ileum in a competitive assay as previously described (30). The *feoB* mutant exhibits a competitive index of 0.46 in vivo and 1.00 in vitro. These data suggest a modest, but statistically significant, in vivo growth defect for the *feoB* mutant. The relatively short infection time (48 h) and the physical ligation of the rabbit intestinal tract in this animal model likely underestimate the importance of FeoB-mediated ferrous iron acquisition for gut colonization, resulting in the observed modest in vivo colonization defect of the *feoB* mutant. Subsequently, to assert the importance of FeoB in vivo and to gain a better understanding of the role of FeoB in the colonization of the host gastrointestinal tract, we compared the capacities of our three *feoB* mutants and wild-type strains of *C. jejuni* to colonize the chick cecum and the piglet gastrointestinal tract. In the chick, where *C. jejuni* is a commensal organism, it does not induce any disease, and it colonizes the cecum at a high level after oral inoculation (20). Consequently, the chick animal model is the model of choice to study *C. jejuni* colonization abilities. However, given the numerous physiological differences between the bird and human gastrointestinal tracts, the information gathered from the colonization of the chick cecum might not be true for the colonization of the mammal intestine during infection. Thus, we also tested the colonization potential of our *C. jejuni* strains in the newborn piglet model of human campylobacteriosis (2). Since the porcine gastrointestinal tract and digestive physiology are very similar to those of humans, the newborn piglet constitutes a good model of human gastroenteritis. In addition, this animal model was previously shown to reproduce clinical outcomes associated with human *Campylobacter* infection (2). In summary, the use of both animals, the chick and the piglet models, should provide valuable information on the role of FeoB in the colonization of the gut during commensal and infectious relationships.

As shown in Fig. 5, the *feoB* mutants of all three strains of *C. jejuni* are significantly affected in their ability to colonize the chick cecum, indicating an important role for ferrous iron acquisition in vivo. The fact that the *feoB* mutants are not entirely inhibited for colonization suggests that they can partially overcome the absence of ferrous iron uptake by acquiring iron from a different source. Analysis of the genome sequence of *C. jejuni* NCTC 11168 reveals that this strain harbors, in addition to the FeoAB ferrous iron transporter, at least two ferric-siderophore transporter systems (CfrA-CeuBCDE for the transport of ferric-enterobactin and Cj0178-Cj0173c/Cj0174c/Cj0175c for the transport of an unknown ferric-siderophore), one hemin transporter system (ChuABCD), and one additional putative iron acquisition system (Cj1658-p19). We have previously shown that the *cfrA*, *ceuE*, and Cj0178 mutants of *C. jejuni* NCTC 11168 were also significantly affected in their ability to colonize the chick cecum, highlighting the importance for siderophore-mediated iron acquisition in vivo (20). Altogether, these data indicate the requirement of both ferric-siderophore and ferrous iron transport systems for the colonization of the chick cecum by *C. jejuni* and suggest that both ferrous and ferric iron sources are available in the intestine. Interestingly, the extent of the colonization defect of the three *feoB* mutants varies significantly between them. The *feoB* mutants of *C. jejuni* NCTC 11168, ATCC 43431, and 81-176 are inhibited for colonization by approximately 20,000-, 50,000-, and 31-fold, respectively. The variation in the colonization defect between the three *feoB* mutants suggests that these strains differ in their iron requirement for in vivo growth and/or in their ability to acquire iron from other sources to overcome the absence of ferrous iron uptake. In agreement with this hypothesis, we and others have previously shown that these three strains of *C. jejuni* harbor a different set of iron uptake systems (8, 23, 24). In fact, the *C. jejuni* ATCC 43431 genome lacks the ferric-enterobactin transporter and *C. jejuni* 81-176 lacks two ferric-siderophore transporter systems (Cj0178 and CfrA). Consequently, whereas ferrous iron appears to be a common iron source for all three strains of *C. jejuni*, the primary source of ferric-siderophore is different between them.

Finally, in order to address the function of FeoB-mediated ferrous iron acquisition for gut colonization in an infectious model of campylobacteriosis, we first established the use of the neonate piglet model to study *Campylobacter* infections with our three wild-type strains, *C. jejuni* NCTC 11168, ATCC 43431, and 81-176. As shown in Table 3, the three wild-type strains of *C. jejuni* colonize the piglets at a level ranging from 10^3 to 10^7 CFU per g of intestinal section on day 3 postinocu-

lation (ca. 10^{10} cells were inoculated orally into each piglet for each bacterial strain). All infected piglets developed diarrhea 12 to 24 h postinoculation. Histological examinations of the intestinal tissues did not reveal any significant pathological lesions. The lack of lesions might simply be a reflection of the fact that the infection period of 3 days was not sufficient to trigger severe inflammation, as previously observed by Babakhani et al. (2). Nevertheless, the induction of diarrhea in pigs infected with each of the three *C. jejuni* strains and the presence of blood in the feces of pigs infected with *C. jejuni* 81-176 and ATCC 43431 indicate that this animal model reproduces the clinical symptoms observed during human infections. The absence of blood in the feces of piglets infected with *C. jejuni* NCTC 11168 suggests that this strain might be less virulent than the two other strains of *C. jejuni*. Given that epithelial cell invasion has been shown to be an important aspect of *Campylobacter* pathogenesis (3), the lower virulence of *C. jejuni* NCTC 11168 would be in agreement with the lower ability of this strain to invade epithelial cells (24). The presence of blood in the feces of the piglets infected with *C. jejuni* 81-176 and ATCC 43431 suggests the existence of histopathological lesions. Strikingly, however, such lesions were not observed. Several causes could explain the lack of lesions. First, the infection period was too short to induce significant lesions. Second, the histopathological lesions occurred at intestinal sections that were not examined and/or the number of intestinal sections examined was insufficient. Third, the occurrence of blood in the stool is the consequence of intestinal hemorrhage by diapedesis upon *C. jejuni* infection.

In the piglet competition assay, each wild-type strain of *C. jejuni* outcompetes its respective *feoB* mutant, indicating that ferrous iron is an important iron source in the pig intestine and that FeoB-mediated iron acquisition is required for *C. jejuni* gut colonization during infectious relationship with its host. The *feoB* mutants of the three strains of *C. jejuni* appear to exhibit different colonization defects (Fig. 7). This outcome likely results from the presence of a different set of iron acquisition systems in these three strains, which is in agreement with the data obtained from the chick colonization assay. Strikingly, the *feoB* mutant of *C. jejuni* ATCC 43431 is more affected in its colonization potential in the duodenum, jejunum, ileum, and colon than in the cecum. In fact, the *feoB* mutant was only recovered in the cecum section of the intestine. In the four other intestinal sections, the number of *feoB* mutant per gram of intestine was below the detection limit of our assay (100 CFU/g). This observation suggests the presence of different iron sources along the gastrointestinal tract and that the *feoB* mutant of *C. jejuni* ATCC 43431 is unable to efficiently acquire these iron sources in the duodenum, jejunum, ileum, and colon sections of the intestine. In contrast, this *feoB* mutant appears to modestly surmount the lack of ferrous iron uptake in the cecum. Given that the colonization of the cecum is higher than in the other intestinal sections, it is tempting to propose that *C. jejuni* ATCC 43431 acquires iron in the cecum from a ferric-siderophore source produced by the indigenous microflora.

In summary, we showed that the *feoB* gene from *C. jejuni* encodes a functional component of the ferrous iron acquisition system. Our data indicate that FeoB provides a selective advantage in the colonization of the host gastrointestinal tract during both commensal and infectious relationships.

In addition, we demonstrated that FeoB plays an essential role for *C. jejuni* intracellular survival. Altogether, the present study highlights the importance of ferrous iron acquisition in the pathogenesis of *C. jejuni*.

ACKNOWLEDGMENTS

We thank I. Turcot for her contribution to the manuscript, C. Picket for strain *C. jejuni* 81-176, A. Labigne for plasmid pILL600, and H. M. Berschneider for the porcine IPEC-1 small intestinal epithelial cells.

This study was supported by National Institutes of Health grant AI055612.

REFERENCES

1. **Andrews, S. C., A. K. Robinson, and F. Rodriguez-Quinones.** 2003. Bacterial iron homeostasis. FEMS Microbiol. Rev. **27:**215–237.
2. **Babakhani, F. K., G. A. Bradley, and L. A. Joens.** 1993. Newborn piglet model for campylobacteriosis. Infect. Immun. **61:**3466–3475.
3. **Bacon, D. J., R. A. Alm, L. Hu, T. E. Hickey, C. P. Ewing, R. A. Batchelor, T. J. Trust, and P. Guerry.** 2002. DNA sequence and mutational analyses of the pVir plasmid of *Campylobacter jejuni* 81-176. Infect. Immun. **70:**6242–6250.
4. **Boyer, E., I. Bergevin, D. Malo, P. Gros, and M. F. Cellier.** 2002. Acquisition of Mn(II) in addition to Fe(II) is required for full virulence of *Salmonella enterica* serovar Typhimurium. Infect. Immun. **70:**6032–6042.
5. **Britton, L., and I. Fridovich.** 1977. Intracellular localization of the superoxide dismutases of *Escherichia coli*: a reevaluation. J. Bacteriol. **131:**815–820.
6. **Dashper, S. G., C. A. Butler, J. P. Lissel, R. A. Paolini, B. Hoffmann, P. D. Veith, N. M. O'Brien-Simpson, S. L. Snelgrove, J. T. Tsiros, and E. C. Reynolds.** 2005. A novel *Porphyromonas gingivalis* FeoB plays a role in manganese accumulation. J. Biol. Chem. **280:**28095–28102.
7. **Day, W. A., Jr., J. L. Sajecki, T. M. Pitts, and L. A. Joens.** 2000. Role of catalase in *Campylobacter jejuni* intracellular survival. Infect. Immun. **68:**6337–6345.
8. **Dorrell, N., J. A. Mangan, K. G. Laing, J. Hinds, D. Linton, H. Al-Ghusein, B. G. Barrell, J. Parkhill, N. G. Stoker, A. V. Karlyshev, P. D. Butcher, and B. W. Wren.** 2001. Whole genome comparison of *Campylobacter jejuni* human isolates using a low-cost microarray reveals extensive genetic diversity. Genome Res. **11:**1706–1715.
9. **Gaynor, E. C., D. H. Wells, J. K. MacKichan, and S. Falkow.** 2005. The *Campylobacter jejuni* stringent response controls specific stress survival and virulence-associated phenotypes. Mol. Microbiol. **56:**8–27.
10. **Grant, A. J., C. Coward, M. A. Jones, C. A. Woodall, P. A. Barrow, and D. J. Maskell.** 2005. Signature-tagged transposon mutagenesis studies demonstrate the dynamic nature of cecal colonization of 2-week-old chickens by *Campylobacter jejuni*. Appl. Environ. Microbiol. **71:**8031–8041.
11. **Hantke, K.** 2004. Ferrous iron transport, p. 178–184. *In* J. H. Crosa, A. R. Mey, and S. M. Payne (ed.), Iron transport in bacteria. ASM Press, Washington, D.C.
12. **Hantke, K.** 1987. Ferrous iron transport mutants in *Escherichia coli* K-12. FEMS Microbiol. Lett. **44:**53–57.
13. **Hu, L., and D. L. Kopecko.** 2005. Invasion, p. 369–383. *In* J. M. Ketley and M. E. Konkel (ed.), *Campylobacter*: molecular and cellular biology. Horizon Bioscience, Norfolk, Va.
14. **Kammler, M., C. Schon, and K. Hantke.** 1993. Characterization of the ferrous iron uptake system of *Escherichia coli*. J. Bacteriol. **175:**6212–6219.
15. **Katoh, H., N. Hagino, A. R. Grossman, and T. Ogawa.** 2001. Genes essential to iron transport in the cyanobacterium *Synechocystis* sp. strain PCC 6803. J. Bacteriol. **183:**2779–2784.
16. **Louvel, H., I. Saint Girons, and M. Picardeau.** 2005. Isolation and characterization of FecA- and FeoB-mediated iron acquisition systems of the spirochete *Leptospira biflexa* by random insertional mutagenesis. J. Bacteriol. **187:**3249–3254.
17. **Marchler-Bauer, A., and S. H. Bryant.** 2004. CD-Search: protein domain annotations on the fly. Nucleic Acids Res. **32:**W327–W331.
18. **Marlovits, T. C., W. Haase, C. Herrmann, S. G. Aller, and V. M. Unger.** 2002. The membrane protein FeoB contains an intramolecular G protein essential for Fe(II) uptake in bacteria. Proc. Natl. Acad. Sci. USA **99:**16243–16248.
19. **Mead, P. S., L. Slutsker, V. Dietz, L. F. McCaig, J. S. Bresee, C. Shapiro, P. M. Griffin, and R. V. Tauxe.** 1999. Food-related illness and death in the United States. Emerg. Infect. Dis. **5:**607–625.
20. **Palyada, K., D. Threadgill, and A. Stintzi.** 2004 Iron acquisition and regulation in *Campylobacter jejuni*. J. Bacteriol. **186:**4714–4729.
21. **Parkhill, J., B. W. Wren, K. Mungall, J. M. Ketley, C. Churcher, D. Basham, T. Chillingworth, R. M. Davies, T. Feltwell, S. Holroyd, K. Jagels, A. V. Karlyshev, S. Moule, M. J. Pallen, C. W. Penn, M. A. Quail, M. A. Rajan-**

dream, K. M. Rutherford, A. H. van Vliet, S. Whitehead, and B. G. Barrell. 2000. The genome sequence of the food-borne pathogen *Campylobacter jejuni* reveals hypervariable sequences. Nature **403:**665–668.
22. **Pesci, E. C., D. L. Cottle, and C. L. Pickett.** 1994. Genetic, enzymatic, and pathogenic studies of the iron superoxide dismutase of *Campylobacter jejuni*. Infect. Immun. **62:**2687–2694.
23. **Poly, F., D. Threadgill, and A. Stintzi.** 2005. Genomic diversity in *Campylobacter jejuni:* identification of *C. jejuni* 81-176-specific genes. J. Clin. Microbiol. **43:**2330–2338.
24. **Poly, F., D. Threadgill, and A. Stintzi.** 2004. Identification of *Campylobacter jejuni* ATCC 43431-specific genes by whole microbial genome comparisons. J. Bacteriol. **186:**4781–4795.
25. **Raphael, B. H., and L. A. Joens.** 2003. FeoB is not required for ferrous iron uptake in *Campylobacter jejuni*. Can. J. Microbiol. **49:**727–731.
26. **Robey, M., and N. P. Cianciotto.** 2002. *Legionella pneumophila feoAB* promotes ferrous iron uptake and intracellular infection. Infect. Immun. **70:** 5659–5669.
27. **Runyen-Janecky, L. J., S. A. Reeves, E. G. Gonzales, and S. M. Payne.** 2003. Contribution of the *Shigella flexneri* Sit, Iuc, and Feo iron acquisition systems to iron acquisition in vitro and in cultured cells. Infect. Immun. **71:**1919–1928.
28. **Stintzi, A.** 2003. Gene expression profile of *Campylobacter jejuni* in response to growth temperature variation. J. Bacteriol. **185:**2009–2016.
29. **Stintzi, A., C. Barnes, J. Xu, and K. N. Raymond.** 2000. Microbial iron transport via a siderophore shuttle: a membrane ion transport paradigm. Proc. Natl. Acad. Sci. USA **97:**10691–10696.
30. **Stintzi, A., D. Marlow, K. Palyada, H. Naikare, R. Panciera, L. Whitworth, and C. Clarke.** 2005. Use of genome-wide expression profiling and mutagenesis to study the intestinal lifestyle of *Campylobacter jejuni*. Infect. Immun. **73:**1797–1810.
31. **Stintzi, A., and L. Whitworth.** 2003. Investigation of the *Campylobacter jejuni* cold shock response to global transcript profiling. Genome Lett. **2:**24–33.
32. **Stojiljkovic, I., M. Cobeljic, and K. Hantke.** 1993. *Escherichia coli* K-12 ferrous iron uptake mutants are impaired in their ability to colonize the mouse intestine. FEMS Microbiol. Lett. **108:**111–115.
33. **Tsolis, R. M., A. J. Baumler, F. Heffron, and I. Stojiljkovic.** 1996. Contribution of TonB- and Feo-mediated iron uptake to growth of *Salmonella typhimurium* in the mouse. Infect. Immun. **64:**4549–4556.
34. **van Vliet, A. H., K. G. Wooldridge, and J. M. Ketley.** 1998. Iron-responsive gene regulation in a *Campylobacter jejuni fur* mutant. J. Bacteriol. **180:**5291–5298.
35. **Velayudhan, J., N. J. Hughes, A. A. McColm, J. Bagshaw, C. L. Clayton, S. C. Andrews, and D. J. Kelly.** 2000. Iron acquisition and virulence in *Helicobacter pylori*: a major role for FeoB, a high-affinity ferrous iron transporter. Mol. Microbiol. **37:**274–286.

Editor: V. J. DiRita